

Behavior of an electron in helium gas

John Bartholomew, Randall Hall, and Bruce J. Berne

Department of Chemistry, Columbia University, New York, New York 10027

(Received 12 March 1985)

A quantum-mechanical electron in dense helium gas is examined by computer simulation using realistic, soft potentials. The behavior of the system is observed as the density is increased; there are indications that the electron (at least partially) localizes and forms a bubblelike state.

The transport properties of an electron in a dense gas have been the subject of much experimental and theoretical investigation.¹⁻²⁷ In helium, as the gas density increases beyond a certain point, the electron mobility is observed to drop faster than the classical rate. While there is not a pure localization phase transition, a change in the dominant character of the system seems clear.

Feynman,¹ Ferrell,² and Kuper³ have suggested that at high He density the electron is trapped inside a bubble. Hiroike, Kestner, Rice, and Jortner⁶ have calculated the radius and energy of this bubble using a soft electron-He pseudopotential. The radius of the bubble is determined by a compromise between the kinetic energy, which delocalizes the electron, the repulsive electron-He potential, which localizes the electron, and the free energy required to form the He-bubble interface. Recently Chandler and co-workers^{25,26} have proposed a mean-field model for electron localization in a system of hard spheres—a model which differs considerably from the pseudopotential model.

We report the results of a path-integral Monte Carlo simulation of an electron in dense He gas as a function of He density using a realistic, "soft" electron-He interaction. Comparison is made with hard-sphere models simulated elsewhere.²⁵⁻²⁷ We perform our study at 77.6 K to make contact with the electric-mobility data of Bartels²⁰ and Schwarz.^{22,23} Our results seem to be consistent with bubble formation.

In the discrete-path representation, the canonical partition function of a quantum-electron-classical-helium system is²⁸

$$Q = \left(\frac{m_e P}{2\pi\hbar^2\beta} \right)^{3P/2} \int d\mathbf{r}_1 \dots d\mathbf{r}_N \int d\mathbf{x}_1 \dots d\mathbf{x}_P \exp(-\beta\Phi), \quad (1)$$

where

$$\Phi \equiv \sum_{i=1}^P \frac{m_e P}{2\hbar^2\beta^2} (\mathbf{x}_i - \mathbf{x}_{i+1})^2 + \frac{1}{P} \sum_{j=1}^N \sum_{i=1}^P V_{e\text{-He}}(|\mathbf{r}_j - \mathbf{x}_i|) + \sum_{j>i} V_{\text{He-He}}(|\mathbf{r}_j - \mathbf{r}_i|), \quad (2)$$

where $\mathbf{r}_1 \dots \mathbf{r}_N$ give the position of N He atoms, $\mathbf{x}_1 \dots \mathbf{x}_P$ give the coordinates of the P -point discretized path of the electron, $\beta = (k_B T)^{-1}$, $V_{e\text{-He}}(|\mathbf{r}_j - \mathbf{x}_i|)$ gives the potential between the discrete-electron point and the j th He atom, and $V_{\text{He-He}}(|\mathbf{r}_j - \mathbf{r}_k|)$ is the interaction potential between the j th and the k th He atoms. The first two terms in Eq. (2) represent the potential energy of a classical cyclic-chain polymer containing particles of mass m_e with nearest-neighbor harmonic bonds. Each bead interacts with each He atom. In the simulation we take $V_{\text{He-He}}(r)$ to be a

Lennard-Jones (LJ) 12-6 potential with $\sigma = 2.576 \text{ \AA}$ and $\epsilon = 10.22 \text{ K}$. $V_{e\text{-He}}(|\mathbf{r}_j - \mathbf{x}_i|)$ is given by the pseudopotential of Kestner, Jortner, Cohen, and Rice.²⁹ The potential is maximum (0.32 a.u.) at a distance $r = 0.61 \text{ \AA}$ and drops by one-half at $r = 1.1 \text{ \AA}$.

The simulation proceeds as follows. The first term on the right-hand side of Eq. (2) can be expressed as $\beta\Phi_e = \sum_k \lambda_k Q_k^2/2$, where Q_k are the normal modes of the chain. We first sample the full set of ($k \neq 0$) normal modes, the step size of mode k being proportional to $\lambda_k^{-1/2}$. The Cartesian coordinates are then calculated and the move accepted or rejected using the Monte Carlo algorithm³⁰ for the full system. The zero-mode translation is made separately. Each He atom is moved separately for the x , y , and z coordinates. Spherical bookkeeping is used.

For our study, the polymer chain has $P = 100$ beads, and the system contains $N = 512$ helium atoms. For many runs, an FPS164 attached processor (AP) was used; one iteration at a helium density of $n = 10^{22} \text{ cm}^{-3}$ takes 4.8 seconds. From 8000 to 15000 passes were made at each density n . Additionally, we made three long runs at $n = 0.9, 1.05,$ and $1.25 \times 10^{22} \text{ cm}^{-3}$ of 75000 passes on a Cray-1; we obtained a factor 8.7 improvement in time over the AP.

The radial-distribution function of He atoms around the electron barycenter

$$g_{e\text{-He}}(r) \equiv \left\langle \delta \left(r - r_{\text{He}} + \frac{1}{P} \sum_{i=1}^P \mathbf{x}_i \right) \right\rangle \quad (3)$$

is determined; this latter quantity is chosen because it can reflect whether or not an electron bubble exists. The non-barycentric, true-distribution function, less suited to signaling bubble formation (where there is no translational invariance) was found not to be as sensitive to changes in density. Also determined are the imaginary-time correlation functions of the form

$$R_n(t-t') \equiv \langle |\mathbf{x}_t - \mathbf{x}_{t'}|^2 \rangle^{1/2} \quad (4)$$

at He density n . These are the root-mean-square displacements between two polymer points separated by a time $(t-t') \in (0, \beta\hbar)$. $R_n(\beta\hbar/2)$ represents the "diameter" of the polymer chain; this quantity is discussed by Chandler and co-workers.^{25,26}

In the simulations reported here, the box-edge length was usually taken to be at least twice the diameter of the polymer. The action Φ was monitored to determine when the system equilibrated. Uncertainties for the quantities measured were determined by blocking the data in successively larger bins until the errors appeared uncorrelated.

Figure 1 shows $R_n(t)$ vs t for various He densities [$R_0(\beta\hbar/2) = 29.2 \text{ \AA}$]. As the density increases, the max-

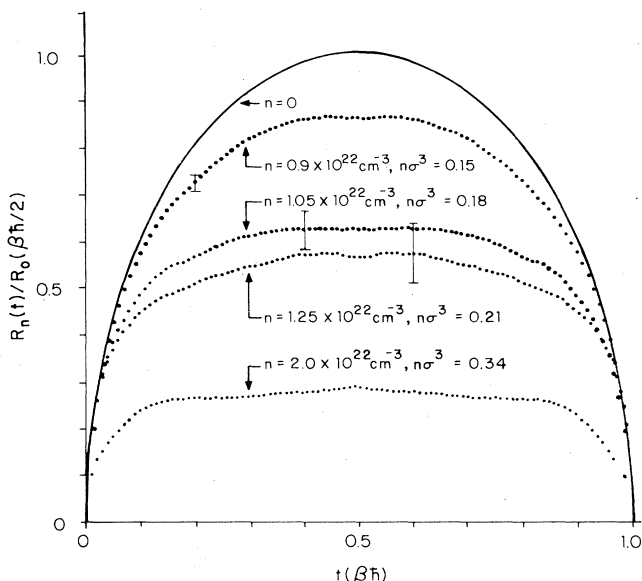


FIG. 1. For the electron-in-helium system at 77.6 K the correlation function $R_n(t)$ vs time t for He densities $n=0, 0.9, 1.05, 1.25$ (all done on the Cray computer), and 2.0 (done on the AP) $\times 10^{22}$ cm^{-3} scaled to the zero-density value $R_0(\beta\hbar/2)$; σ is the He-He LJ parameter. The error bars shown are typical (the ones for $n=2.0 \times 10^{22}$ cm^{-3} are too small to show).

imum at $t = \beta\hbar/2$ decreases and the curve levels off faster; the polymer chain goes from a free, extended state to a compact, quasilocated state showing signs of ground-state dominance.^{25,26}

Figure 2 shows $R_n(\beta\hbar/2)$ versus density n . Initially, the decrease is slow. The most rapid decrease is around $n = 1.0 \times 10^{22}$ cm^{-3} (corresponding to $n\sigma^3 = 0.17$, where σ is the LJ parameter); there is a slower decrease at high densities. For the AP points, error bars cannot be as confidently determined due to there being fewer passes. We show these data without error bars, the scatter in the points themselves giving a measure of error. One should not read fine structure into the $R_n(\beta\hbar/2)$ vs n curve; the curve drawn to guide the eye shows the general trend of the data. The

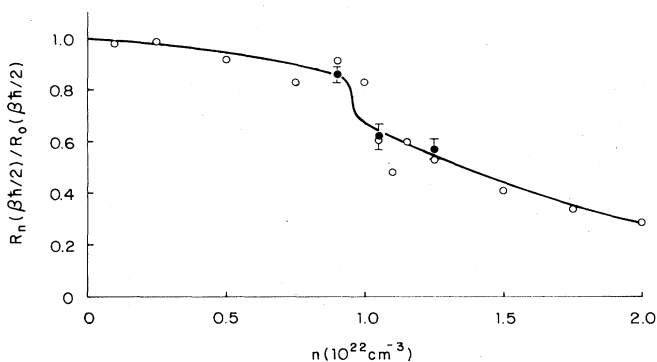


FIG. 2. The electron-polymer extent $R_n(\beta\hbar/2)$, scaled to the zero-density value, vs density n . Data obtained with the Cray computer are plotted as closed circles, data obtained with the AP as open circles. The curve is drawn to guide the eye.

Cray runs give high-precision data showing more specifically the shape of the curve and act as a standard for the AP runs.

At $n = 1.25 \times 10^{22}$ cm^{-3} , the polymer behaved as if the electron were localized for 4×10^4 passes with $R_n(\beta\hbar/2)/R_0(\beta\hbar/2) = 0.44 \pm 0.02$ and then shifted to a quasifree state for about 10^4 passes with $R_n(\beta\hbar/2)/R_0(\beta\hbar/2) = 1.02 \pm 0.01$. This shows the electron enters a region where the gas is locally rarefied and remains there metastably.

We may extract a bubble radius $R = \frac{1}{2}R_n(\beta\hbar/2) \approx (4 \pm 1)$ Å at high density. This is in excellent agreement with the value $R \approx 4.2$ Å given by Jahnke and Silver¹⁹ for He gas at a temperature $T = 77.3$ K, nearly the temperature used in our simulation. For liquid He at $T = 0$ K, Hiroike *et al.*⁶ concluded $R = 12.4$ Å. For the gas at $T \approx 4.2$ K the following values were obtained: $R \approx 16$ Å by Levine and Sanders,⁷ $R \approx 16$ Å by Young,¹¹ $R \approx (6-15)$ Å by Eggarter and Cohen,¹² $R \approx 14$ Å by Eggarter,¹⁵ $R \approx 16$ Å by Schwarz.²³ While Jahnke and Silver considered their value low given the liquid-He values, it is quite reasonable considering that the bubble radius and other quantum-mechanical wavelengths will generally scale as $1/T^{1/2}$.

Our results for a realistic simulation of the physical system contrast with hard-sphere results;²⁵⁻²⁷ differences in results are expected because use of hard spheres is a simplifying approximation. Comparison with Chandler and co-workers^{25,26} shows our dropoff in $R_n(\beta\hbar/2)$ to be more rapid and preceded by a more constant-density shoulder; the $R_n(\beta\hbar/2)$ vs n curve is of different character.³¹ In Ref. 25, mean-field, adiabatic, polaron, and nonpolarization approximations are used. We tested the Gaussian hypothesis used which asserts $\langle |x_{t+s} - x_t|^4 \rangle / \langle |x_{t+s} - x_t|^2 \rangle^2 = \frac{5}{3}$. For various separations s , at $n = 1.05, 1.25$, and 1.5×10^{22} cm^{-3} , this ratio was evaluated and found to agree with $\frac{5}{3}$ within errors, but the values without the uncertainties show an increasing trend as s goes from 0 to $\beta\hbar/2$, indicating possible higher-order effects.

Our decrease in $R_n(\beta\hbar/2)$ with n is slower than that for a rigid, disordered configuration of hard spheres considered by Sprik, Klein, and Chandler.²⁷ This is very likely a result of their much greater implied temperature which would result in considerable density-scale compression. For a reasonable value of the electron-He distance of closest approach, the implied temperature is several hundred degrees.³² Further, the general shapes of the curves are different, there again being the absence of a shoulder.

Figures 3 show the electron-He radial distribution functions $g_{e-\text{He}}(r)$ taken from the polymer barycenter at four densities.³³ As the density increases, He atoms are excluded from the volume occupied by the polymer, resulting in the bubble. At $n = 2.0 \times 10^{22}$ cm^{-3} , we may again read off a bubble radius of $R \approx (5 \pm 1)$ Å, consistent with our earlier determination.

Note that there may be "asynchronization" of static and dynamic properties of the system. The data of Bartels²⁰ show a much stronger decrease in mobility by $n = 0.5 \times 10^{22}$ cm^{-3} than any of the static quantities measured here would indicate: there seems to be a "lag" between static and dynamic measurements. This implication holds also for Ref. 26. As the statics are already difficult, the dynamics will not be easily addressed.

What of the reliability of our data?

(1) *Thermalization.* Data were averaged only after the ac-

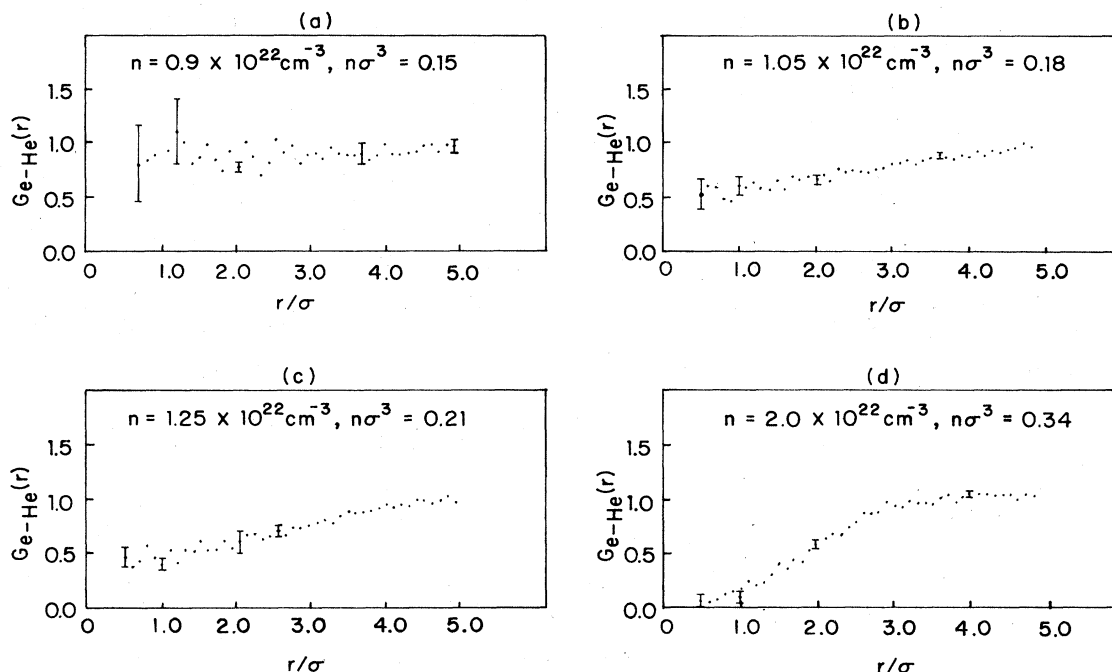


FIG. 3. The electron-helium radial-distribution function $g_{e\text{-He}}(r)$ vs distance r , taken with respect to the polymer barycenter at four densities: (a) $n=0.9$, (b) 1.05, (c) 1.25, and (d) $2.0 \times 10^{22} \text{ cm}^{-3}$. The first three are data from the Cray; the last is data from the AP. σ is the He-He LJ parameter. The error bars shown are typical.

tion thermalized. This took about 10^3 passes at low densities and up to 6×10^3 at high densities. We note that certain initial configurations do not thermalize easily because of metastable trapping of polymer beads in a He cluster.

(2) *Fluctuations.* Once the system thermalized, quantities averaged have fluctuations on short Monte Carlo time scales, but values of $R_n(\beta\hbar/2)$ can show fluctuations on the order of 5000 or more passes [especially where $R_n(\beta\hbar/2)$ decreases rapidly with density]. However, the Cray runs which averaged many cycles agree with AP runs which averaged few—there is some degree of similarity in the large cycles. Outside the region of the “transition,” at high and low densities, fluctuations are less serious and the AP data are reliable.

(3) *Number of polymer beads.* This study used $P=100$ beads, a constraint imposed by computer memory and running time. A run of 4×10^4 passes with $P=500$ was made at $n=1.25 \times 10^{22} \text{ cm}^{-3}$ with 2×10^4 passes required for equilibration. Because fewer passes could be made than for the $P=100$ case, the quasifree state was never sampled. A value of $R_n(\beta\hbar/2)/R_0(\beta\hbar/2) = 0.39 \pm 0.01$ was obtained, in reasonable agreement with the $P=100$ value of 0.44 ± 0.02 for the localized state. There could be some sharpening of the initial rise in $R_n(t)$ vs t and a lowering of $R_n(\beta\hbar/2)$ for

n in the localized regime as P increases, but we do not expect this to change our results significantly.

We have treated the He classically; its free-polymer radius would be 0.34 Å. A more refined calculation should consider the quantum nature of He. We do not expect such quantum effects to be important.

(4) *System size.* Finite-size studies at lower densities showed that maintaining the box edge at two to three times $R_n(\beta\hbar/2)$ was adequate. We point out that an extremely small box could give anomalously strong nonlocal bead interactions mediated by the He due to the periodic boundary conditions.

The electron-in-helium system is an intriguing one and remains difficult to probe. We hope these results—though not final ones³⁴—contribute to the understanding of that system.

We acknowledge M. Herman, K. Schwarz, D. Thirumalai, and A. Wallqvist for helpful discussions. This work was supported by grants from the National Science Foundation (NSF), the NSF Supercomputer Division, and the National Institutes of Health. Without the help of the Supercomputer Division this study could not have been done reliably.

¹R. P. Feynman (unpublished), reported in C. G. Kuper, *Phys. Rev.* **122**, 1007 (1961).

²R. A. Ferrell, *Phys. Rev.* **108**, 167 (1957).

³C. G. Kuper, Ref. 1.

⁴J. Levine and T. M. Sanders, Jr., *Phys. Rev. Lett.* **8**, 159 (1962).

⁵J. Jortner, N. R. Kestner, S. A. Rice, and M. H. Cohen, *J. Chem. Phys.* **43**, 2614 (1965).

⁶K. Hiroike, N. R. Kestner, S. A. Rice, and J. Jortner, *J. Chem. Phys.* **43**, 2625 (1965).

⁷J. L. Levine and T. M. Sanders, Jr., *Phys. Rev.* **154**, 138 (1967).

- ⁸J. M. Ziman, *J. Phys. C* **1**, 1532 (1968).
- ⁹H. E. Neustadter and M. H. Coopersmith, *Phys. Rev. Lett.* **23**, 585 (1969).
- ¹⁰T. P. Eggarter and M. H. Cohen, *Phys. Rev. Lett.* **25**, 807 (1970).
- ¹¹R. A. Young, *Phys. Rev. A* **2**, 1983 (1970).
- ¹²T. P. Eggarter and M. H. Cohen, *Phys. Rev. Lett.* **27**, 129 (1971).
- ¹³H. R. Harrison and B. E. Springett, *Phys. Lett.* **35A**, 73 (1971).
- ¹⁴J. P. Hernandez, *Phys. Rev. A* **5**, 635 (1972).
- ¹⁵T. P. Eggarter, *Phys. Rev. A* **5**, 2496 (1972).
- ¹⁶H. R. Harrison, L. M. Sander, and B. E. Springett, *J. Phys. B* **6**, 908 (1973).
- ¹⁷J. P. Hernandez and J. M. Ziman, *J. Phys. C* **6**, L251 (1973).
- ¹⁸J. P. Hernandez, *Phys. Rev. A* **7**, 1755 (1973).
- ¹⁹A. Jahnke and M. Silver, *Chem. Phys. Lett.* **19**, 231 (1973).
- ²⁰A. Bartels, *Appl. Phys.* **8**, 59 (1975).
- ²¹J. A. Jahnke, M. Silver, and J. P. Hernandez, *Phys. Rev. B* **12**, 3420 (1975).
- ²²K. W. Schwarz, *Phys. Rev. Lett.* **41**, 239 (1978).
- ²³K. W. Schwarz, *Phys. Rev. B* **21**, 5125 (1980).
- ²⁴M. Parrinello and A. Rahman, *J. Chem. Phys.* **80**, 860 (1984).
- ²⁵D. Chandler, Y. Singh, and D. M. Richardson, *J. Chem. Phys.* **81**, 1975 (1984).
- ²⁶A. L. Nichols III, D. Chandler, Y. Singh, and D. M. Richardson, *J. Chem. Phys.* **81**, 5109 (1984).
- ²⁷M. Sprik, M. L. Klein, and D. Chandler, *Phys. Rev. B* **31**, 4234 (1985).
- ²⁸R. P. Feynman and A. R. Hibbs, *Quantum Mechanics and Path Integrals* (McGraw-Hill, New York, 1965).
- ²⁹N. R. Kestner, J. Jortner, M. H. Cohen, and S. A. Rice, *Phys. Rev.* **140**, A56 (1965). This potential is valid only at zero momentum, but we do not expect this to be a relatively large source of error.
- ³⁰N. Metropolis, A. W. Rosenbluth, M. N. Rosenbluth, A. H. Teller, and E. Teller, *J. Chem. Phys.* **21**, 1087 (1953).
- ³¹There are some difficulties in making the comparison. In Refs. 25 and 26, the diameter of the solvent molecule, σ , is taken equal to twice the distance of closest approach of the electron to a solvent sphere, $2d$. If we identify σ with the LJ sigma parameter, we have $\sigma = 2.6$ Å. Choosing d from the electron-He pseudopotential is problematic; $d \approx 2.1$ Å seems reasonable. With a choice of $\sigma = 2.4$ Å as a compromise, for the temperature 77.6 K, one has $\lambda_e/\sigma = 14.2$ in Fig. 5 of Ref. 26. (There, $\rho\sigma^3 = 1$ means $\rho = 7.4 \times 10^{22}$ cm⁻³.)
- ³²In Fig. 5 of Ref. 27, there is a 35% decrease in $R(\beta\hbar/2)$ from $n = 0$ to 1.05×10^{22} cm⁻³, taking the electron-He distance of closest approach $\sigma/2 \approx 1.1$ Å; the temperature for our problem is 548 K.
- ³³We do not attempt to smooth these data since only one electron is being considered.
- ³⁴We have also made runs on this system using Fourier-coefficient Monte Carlo. See Ref. 28, and W. H. Miller, *J. Chem. Phys.* **63**, 1166 (1975); J. D. Doll and D. L. Freeman, *ibid.* **80**, 2239 (1984); J. D. Doll, *ibid.* **81**, 3536 (1984). To obtain correlation functions, we found out that on the order of a hundred Fourier coefficients were required. The time per iteration is very much slower and metastable traps are not avoided, calling into question the efficacy of this method for the electron-in-helium problem.